

Effects of intrinsic threedimensionality on the drag characteristics of a normal flat plate

F. M. Najjar and S. P. Vanka

Citation: [Physics of Fluids \(1994-present\)](#) **7**, 2516 (1995); doi: 10.1063/1.868698

View online: <http://dx.doi.org/10.1063/1.868698>

View Table of Contents: <http://scitation.aip.org/content/aip/journal/pof2/7/10?ver=pdfcov>

Published by the [AIP Publishing](#)

Articles you may be interested in

[Three-dimensional instability in flow past a rectangular cylinder ranging from a normal flat plate to a square cylinder](#)

Phys. Fluids **26**, 061702 (2014); 10.1063/1.4883176

[Phaselocked eduction of vortex shedding in flow past an inclined flat plate](#)

Phys. Fluids **8**, 1159 (1996); 10.1063/1.868907

[Details of the drag curve near the onset of vortex shedding](#)

Phys. Fluids **7**, 2102 (1995); 10.1063/1.868459

[Threedimensional vorticity modes in the wake of a flat plate](#)

Phys. Fluids A **2**, 371 (1990); 10.1063/1.857787

[Instability and transition of a threedimensional boundary layer on a swept flat plate](#)

Phys. Fluids **31**, 786 (1988); 10.1063/1.866814



Effects of intrinsic three-dimensionality on the drag characteristics of a normal flat plate

F. M. Najjar^{a)}

National Center for Supercomputing Applications, University of Illinois at Urbana—Champaign,
5600 Beckman Institute, 405 North Mathews, Urbana, Illinois 61801

S. P. Vanka^{b)}

Department of Mechanical and Industrial Engineering, University of Illinois at Urbana—Champaign,
Urbana, Illinois 61801

(Received 2 March 1995; accepted 31 May 1995)

A three-dimensional direct numerical simulation of the wake of a flat plate held normal to a free stream has been conducted for a Reynolds number of 1000, using a high-order finite-difference scheme. The calculated flow structures and the coefficient of drag are shown to be markedly different from those obtained from an equally resolved two-dimensional simulation. The three-dimensional simulation is able to account for the intrinsic three-dimensionality that develops beyond a certain critical Reynolds number (~ 200). The time-averaged drag predicted by the three-dimensional simulation is in good agreement with the experimental data, and also captures a low-frequency time variation that is seen in the experiments. © 1995 American Institute of Physics.

A common assumption in almost all simulations of bluff body wakes has been that the instantaneous, as well as the time-mean flow fields, are two dimensional. This has been a matter of necessity, because accurate resolution of a three-dimensional flow is computationally expensive. Comparisons of the calculated drag and lift coefficients, as well as the vortex shedding frequency with available data¹ were satisfactory, but were not excellent, because of the inadequate resolution of the wake features. However, such three-dimensional effects become important, even at very modest Reynolds numbers, leading to highly complex flow structures and associated time-dependent pressure and velocity fields.

It is essential to first recognize that there are two types of three-dimensionality.² The first type is called “extrinsic” and is caused by variations of the body shape and (or) the boundary conditions in all three spatial directions. This type can be contrasted with “intrinsic” three-dimensionality that arise when secondary instabilities are generated in an initially two-dimensional flow. Such is the case for wakes of two-dimensional bodies above a certain critical Reynolds number. The critical Reynolds number for the onset of intrinsic three-dimensionality varies with the geometry, but is in the proximity of 200. When such three-dimensionality arises, there can be significant spanwise variations in the velocity and pressure fields, as well as the drag and lift coefficients. It is well recognized in the literature on mixing layers and shear layers that such three-dimensionality is associated with regions of streamwise vorticity called “ribs” that are connected in a complicated manner with the main “rollers.”³ The rollers themselves are also distorted in the spanwise direction because of these secondary instabilities. Similar structures were also observed in bluff body wakes⁴ and influence the drag considerably. For a flat plate held normal to a free stream, the measured drag coefficient is around 2.0.⁵ Simulations that assume a two-dimensional flow are unable to predict this value.^{6,7} This discrepancy is less severe for other geometries.^{8,9}

We have recently completed a three-dimensional (3-D)

direct numerical simulation (DNS) of the wake of a normal flat plate with zero thickness. A high-order finite-difference numerical procedure has been used to simulate the flow at a Reynolds number ($U_\infty h/\nu$) of 1000. Complete details of the numerical procedure, its implementation, and performance on a parallel computer, and time-averaged statistics are given in the thesis of Najjar.⁷ Briefly, the numerical procedure uses a combination of fourth- and fifth-order differencing schemes for several of the partial derivatives and a control volume formulation of the mass continuity equation. The pressure Poisson equation arising out of the fractional step method is solved with a direct procedure, in conjunction with a Capacitance Matrix technique. A nonuniformly placed finite-difference grid of $256 \times 256 \times 32$ nodes was used to resolve the flow on a computational domain of $-8 \leq x \leq 20$; $-8 \leq y \leq 8$ and $0 \leq z \leq 2\pi$. In the spanwise (z) direction, periodic conditions are used. The period 2π is several times larger than the distance between two consecutive streamwise ribs, and adequately resolves the 3-D structures. The adequacy of the spanwise grid resolution was ensured through a five order reduction of the spanwise Fourier coefficients of pressure. The Reynolds number of 1000 is considerably higher than the critical Reynolds number for secondary instability, and is selected as a “safe” Reynolds number to well establish the features of the intrinsic three-dimensionality and its effect on the overall drag coefficient. The simulation was integrated for 170 nondimensional time units, where seven time units approximately represent one vortex shedding cycle. History of the pressure signals and the averaged drag coefficient revealed considerable departure from similar results of a two-dimensional simulation.

We first show in Fig. 1(a) one instantaneous snapshot of the contours of spanwise vorticity ($\omega_z = \partial v/\partial x - \partial u/\partial y$) obtained from the 3-D simulation at one of the x - y planes and contrast it, in Fig. 1(b), with that obtained from a 2-D simulation. The negative spanwise vorticity corresponds to clockwise rotation of the vortices and the positive vorticity corresponds to counterclockwise rotation. The grid resolution in

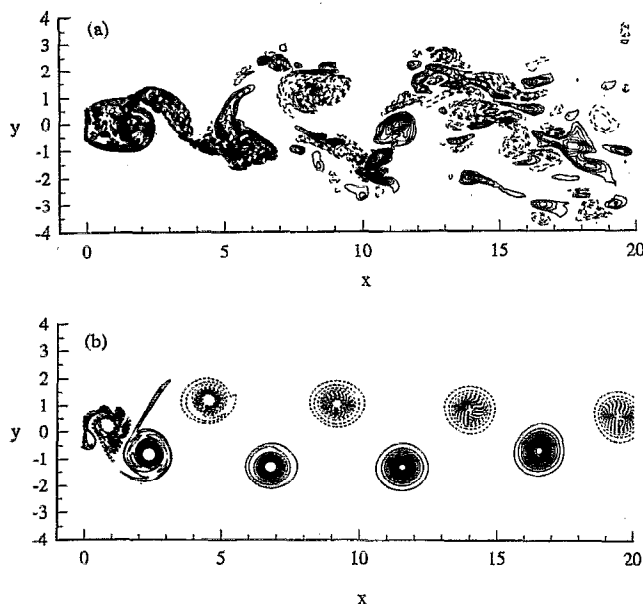


FIG. 1. Contours of instantaneous spanwise vorticity for flow over a normal flat plate at $Re=1000$ computed from (a) 3-D simulation and (b) 2-D simulation. Dashed lines represent negative values.

the 2-D simulation was similar to that in the 3-D simulation. Note that in the 3-D simulation, there are 32 planes, and we have displayed the flow field in only one of these planes. The first striking difference between the two snapshots is the structure of the shear layers developing from the edges of the plate. In the 3-D simulation, the shear layer is seen to extend up to two plate heights before rolling up into vortices. In the 2-D results, the shear layers roll up closer to the plate. Further, in the 3-D simulation, the vortices quickly break up into smaller vortices after an x of 8.0, whereas the 2-D results show no such breakup. In the 2-D simulations, distinct and strong vortices are observed to convect parallel to the centerline for a considerable distance and to then converge toward the centerline around $x=14$. The converging vortices are observed to subsequently pair and interact with each other before being convected out of the computational domain.¹⁰ The absence of vortex stretching and tilting in the spanwise direction prevents any distortion of the rollers. Although some fine-scale structures are observed in the very near region of the plate, these eventually combine and form more coherent spanwise vortices at an x of 5.

Figure 2 presents a 3-D perspective of the surface of streamwise vorticity ($\omega_x = \partial w / \partial y - \partial v / \partial z$) of value $+2.5$ units. This figure reveals the formation of “rib”-like structures between two adjacent spanwise rollers. These ribs occur in pairs of opposite vorticity. The origin of these ribs can be traced to the shear layer, which, due to secondary instabilities, first produces regions of concentrated streamwise vorticity. When a spanwise roller is shed from this shear layer, these regions of streamwise vorticity become organized into elongated structures, which then attach themselves to the previously shed roller. Thus, rollers of opposite spanwise vorticity are connected by these ribs in an alternate “top-to-top” and “bottom-to-bottom” fashion. The ribs originating in the lower shear layer connect two rollers at



FIG. 2. A 3-D perspective view of the instantaneous streamwise vorticity for flow over a normal flat plate at $Re=1000$. Surface level: $\omega_x = +2.5$.

their tops, while the ribs originating from the upper shear layer connect the bottoms of the rollers. This topology is similar to that conjectured by Hussain and Hayakawa¹¹ for the turbulent wake of a circular cylinder. The region where the ribs are attached to the rollers has been previously termed as the “braid region.”

The effect of this intrinsic three-dimensionality is reflected in marked differences in the time variation, as well as the magnitude of the span-averaged drag coefficient. Figure 3 shows the time variation of the drag coefficient from 2-D and 3-D simulations. There are again significant differences between the two results. First, as also observed by earlier investigators, the 2-D simulation considerably overpredicts the drag coefficient. The value from the 3-D computation is closer to the experimental value of 1.84 of Fage and Johansen.⁵ Further, the 2-D drag exhibits a periodic time variation reflecting the vortex shedding process, while in the 3-D simulation the spanwise integration of the force difference produces a more uniform time signature. The 3-D simulation also reveals a low frequency, with a period of about six to seven times that of the main vortex shedding. It is interesting to note that such a low frequency has been observed also in experiments.¹² Tafti and Vanka¹³ have observed a similar low frequency in a 3-D simulation of the separated

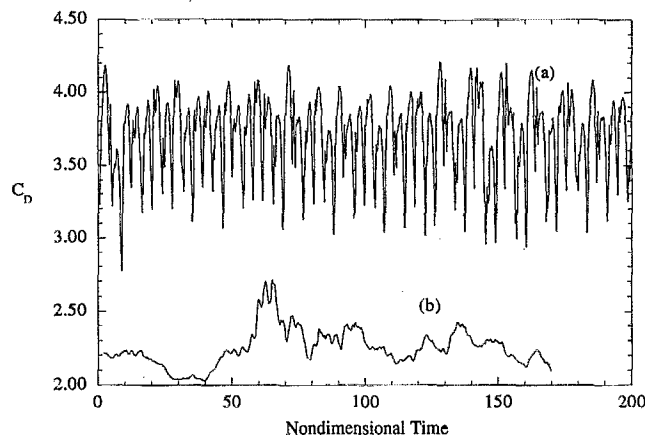


FIG. 3. Time trace of the instantaneous drag coefficient at $Re=1000$, calculated by (a) 2-D simulation and (b) 3-D simulation.

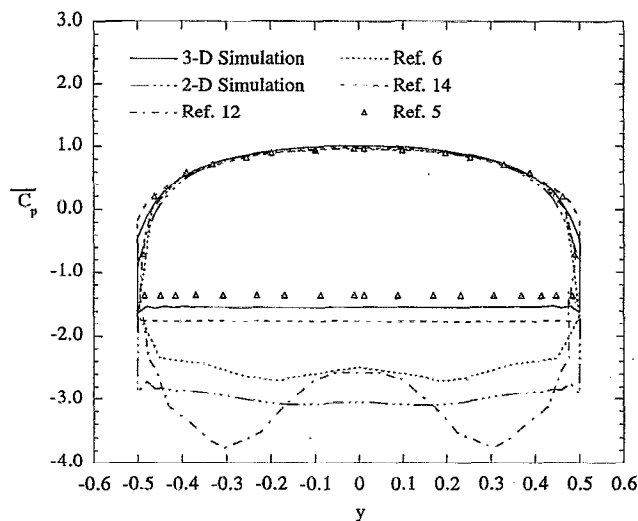


FIG. 4. Distribution of the mean surface pressure coefficient, \bar{C}_p , on the front and rear sides of the flat plate.

and reattaching flow over a blunt plate, and attributed it to a low-frequency flapping of the shear layer. Whether the low frequency observed in the wake of a flat plate is of a similar nature can only be speculated at this time.

Finally, in Fig. 4, we present the distribution of the mean pressure coefficient \bar{C}_p , on the surface of the plate. Also presented here are experimental data of Fage and Johansen⁵ and previous computational results.^{6,12,14} Of all these results, the current 3-D simulation comes closest to the experimental data. The 2-D finite difference,¹⁴ as well as the discrete vortex^{6,12} simulations do not capture the “flat” distribution of the pressure on the rear side of the plate, as observed in the experiments. This variation is, however, well captured by the 3-D simulation. The mean drag coefficient (averaged over the last 15 cycles) predicted by the current 3-D simulation is 2.26. However, if we use Maskell’s formula¹⁵ to correct for blockage effects caused by the finite computational domain, the drag reduces to 1.99 (for $\epsilon=0.066$). This compares closely with the experimental values of 1.84,⁵ 1.89,¹⁶ and 1.88.⁶ Note that the inclusion of leakage effects in the experiments can slightly increase the drag coefficient, as pointed out by Abernathy.¹⁷

In summary, a three-dimensional direct numerical simulation has been performed to quantify the effects of the “intrinsic” three-dimensionality on the drag and flow characteristics of the wake of a normal flat plate. The 3-D simulation

is able to capture the existence of regions of streamwise vorticity in the form of ribs connecting adjacent Karman vortex rollers. With the inclusion of the 3-D effects, the values of the mean pressure coefficient and the drag are in close agreement with the experimental data. It is clear that the intrinsic 3-D effects that evolve at higher Reynolds numbers are important for this flow configuration, and must be included in a numerical simulation, although the geometry is nominally two dimensional.

ACKNOWLEDGMENT

This work was supported by the ONR, NSF, and NCSA.

^{a)}Tel.: (217) 244-3282; fax: (217) 244-2909; e-mail: najjar@ncsa.uiuc.edu.

^{b)}Tel.: (217) 244-8388; fax: (217) 244-6534; e-mail: vanka@spvindigo.me.uiuc.edu.

¹S. F. Hoerner, *Fluid-Dynamic Drag* (Hoerner Fluid Dynamics, Brick Towns, NJ, 1965).

²A. Roshko, “Perspectives on bluff body aerodynamics,” *J. Wind Eng. Ind. Aerodyn.* **49**, 79 (1993).

³G. Brown and A. Roshko, “On density effects and large structure in turbulent mixing layers,” *J. Fluid Mech.* **64**, 775 (1974).

⁴H. L. Grant, “Large eddies of turbulent motion,” *J. Fluid Mech.* **4**, 149 (1958).

⁵A. Fage and F. C. Johansen, “On the flow of air behind an inclined flat plate of infinite span,” British Aero Research Council 1104, 1927.

⁶D. Lisoski, “Nominally two-dimensional flow about a normal flat plate,” Ph.D. thesis, California Institute of Technology, 1993.

⁷F. M. Najjar, “Direct numerical simulations of separated and separated-reattaching flows on massively parallel processing computers,” Ph.D. thesis, University of Illinois at Urbana—Champaign, 1994.

⁸T. Tamura, I. Ohta, and K. Kuwahara, “On the reliability of two-dimensional simulation for unsteady flows around cylinder-type structure,” *J. Wind Eng. Ind. Aerodyn.* **35**, 275 (1990).

⁹R. Mittal and S. Balachandar, “Effect of three-dimensionality on the lift and drag of circular and elliptic cylinders,” submitted for publication.

¹⁰F. M. Najjar and S. P. Vanka, “Simulations of the unsteady separated flow past a normal flat plate,” *Int. J. Num. Methods Fluids* (accepted).

¹¹F. Hussain and H. Hayakawa, “Eduction of large scale organized structures in a turbulent plane wake,” *J. Fluid Mech.* **180**, 193 (1987).

¹²K. Chua, D. Lisoski, A. Leonard, and A. Roshko, “A numerical and experimental investigation of separated flow past an oscillating flat plate,” *ASME Nonsteady Flow Symp. FED 92*, 455–464 (1990).

¹³D. K. Tafti and S. P. Vanka, “A three-dimensional numerical study of flow separation and reattachment on a blunt plate,” *Phys. Fluids A* **3**, 2887 (1991).

¹⁴D. S. Joshi, S. P. Vanka, and D. K. Tafti, “Large eddy simulation of the wake of a normal flat plate,” *Boundary Layers and Free Shear Flows*, (ASME, New York, 1994), FED 184, p. 231.

¹⁵E. C. Maskell, “A theory of the blockage effects on bluff bodies and stalled wings in a closed wind tunnel,” *Aerospace Research Communications Report Memo*, 3400, 1963.

¹⁶I. P. Castro, “Wake characteristics of two-dimensional perforated plates normal to an airstream,” *J. Fluid Mech.* **46**, 599 (1971).

¹⁷F. H. Abernathy, “Flow over an inclined plate,” *Trans. ASME J. Basic Eng.* **61**, 380 (1962).